Journal of Electronic Materials, Vol. 9, No. 3, 1980

THE PREPARATION OF $Ga_{1-x}In_xAs$ BY ORGANOMETALLIC PYROLYSIS FOR HOMOJUNCTION LED'S

J.P. Noad and A.J. SpringThorpe

BELL-NORTHERN RESEARCH
P.O. Box 3511, Station C
Ottawa, Ontario, Canada

(Received November 13, 1979)

$Ga_{1-x}In_xAs$ epitaxial layers have been deposited on GaAs substrates using the technique of organometallic pyrolysis (metalorganic chemical vapour deposition). The deposition was performed in a laminar flow, resistively heated, reactor. Both n and p-type (10^{17}-10^{18} carriers/cm^3) epitaxial layers, several microns thick,were prepared, with values of x in the range $0 \leq x \leq 0.3$. Epitaxial layer characterisation was carried out using conventional electrical, optical and x-ray techniques. Restricted emitting area (50-75 μm diameter) zinc-diffused LED's were prepared in ungraded epitaxial layers with emission spectral peaks in the range 0.9 - 1.15 μm. External quantum efficiencies of these devices decreased rapidly with increasing x, from ~0.4% for GaAs LED's to ~0.02% for $Ga_{0.75}In_{0.25}As$ LED's.

Key words: Organometallic pyrolysis, Metalorganic CVD
$Ga_{1-x}In_xAs$, Epitaxial growth, LED's.

Introduction

There is considerable current interest in the development of semiconductor materials for device applications for long-wavelength optical-fibre communication systems (1).

0361-5235/80/0500-0601$03.00/1

Both ternary and quaternary III-V compound alloys can be tailored to produce the required device materials, with optoelectronic properties appropriate to specific wavelength ranges (2). In this area the major concentration of effort for light sources is on the development of p-n junction lasers based on lattice-matched GaInAsP quaternary alloys (3). LED's made from this (4) and other alloy systems can offer some short term advantages, particularly in the area of device reliability. Alternative alloys for LED and detector applications can be formed from the ternary system Ga-In-As, and devices made from this ternary can, in principle, cover the wavelength range 0.9 - 3.4 μm. In recent years both high intensity LED's, 1.06 μm emission (5), and efficient avalanche photodiodes, sensitive in the range 1.0 - 1.6 μm (6), have been reported. This ternary alloy system is the subject of the present investigation.

Epitaxial layers of $Ga_{1-x}In_xAs$, suitable for device applications, have been prepared on GaAs substrates by chemical vapour deposition (CVD) (5), molecular beam epitaxy (7), and liquid-phase epitaxial (LPE) techniques (8). Because of the lattice-mismatch between the $Ga_{1-x}In_xAs$ and the substrate ($\Delta a/a \sim 2\%$ for $x \sim 0.3$) it is generally necessary to grade the epitaxial layer to its final required composition in order to minimise the dislocations generated by the mismatch. Although this is relatively easy to accomplish with the CVD technique, it is difficult with LPE. Unfortunately, CVD requires the simultaneous control of a number of independent temperature zones in the deposition furnace and is generally more complex than LPE. However, the more recently developed vapour phase technique based upon organometallic pyrolysis (OMP) (9) retains the capability to control the composition of the epitaxial layer, while only requiring the control of one heated zone. Furthermore, since there is no requirement for equilibration of the carrier gas system with heated sources, sharper compositional changes should be possible than with CVD.

Since the pioneering work of Manasevit (9) on OMP, its potential for the production of high quality III-V compounds and alloys has been convincingly demonstrated. Device quality material for such diverse applications as GaAs FET's (10), GaAlAs-GaAs solar cells (11,12) and GaAlAs DH lasers (13,14) has been produced in recent years.

In this paper we report the results of the preparation of $Ga_{1-x}In_xAs$ ($x \leq 0.3$) epitaxial layers on GaAs substrates by OMP. These layers have been used in the preparation and evaluation of homojunction LED's emitting in the wavelength range 0.9 - 1.15 μm.

Materials Preparation

a) Organometallic Pyrolysis (OMP) Deposition System

The basic reaction used in the organometallic pyrolysis deposition of III-V semiconductors involves the simultaneous thermal decomposition of an organometallic compound containing a group III element (e.g. Trimethylgallium; TMG) together with a group V hydride (e.g. Arsine; AsH_3) in a gaseous environment (15). Chemically the reaction for the formation of GaAs by the pyrolysis of TMG and AsH_3 can be written as:

$$(CH_3)_3Ga + AsH_3 \longrightarrow GaAs\downarrow + 3CH_4\nearrow \qquad (1)$$

Similar reactions can be written for the formation of most of the III-V compounds, but the necessary gas phase concentrations and decomposition temperatures for optimal epitaxial growth will vary from compound to compound. Of particular interest, however, is the situation when there is more than one group III organometallic present in the deposition zone, since this enables III-V compound alloys to be formed. By varying the relative concentrations of the two elements in the gaseous phase one can, in principle, vary the resulting alloy compositions at will throughout the whole of an alloys existence range. In practice, competing side reactions, ignored in Eq. 1, may limit the range of alloys that can be easily prepared. The work reported in this paper follows from the initial work of Manasevit (16) and Baliga and Ghandi (17) on the GaAs-InAs alloy system. Triethylindium (TEI) and TMG were used as the sources of group III elements, which together with AsH_3, enabled a range of $Ga_{1-x}In_xAs$ alloys to be prepared. A schematic of the apparatus used is shown in Figure 1. TMG and TEI vapour were picked up by high purity Pd-diffused hydrogen which was bubbled through the liquid, semiconductor grade* organometallics. Because of the high vapour pressure of TMG it was necessary

*Alfa-Ventron Corporation

to cool its bubbler to 0°C. Even with this cooling, however, very low gas flows were required (1-3 cm^3/min), which necessitated the use of mass-flow controllers to ensure reproducible growth rates and alloy compositions. Since the vapour pressure of TEI is low at 300K, much higher carrier gas flow rates were required (100-500 cm^3/min) and its bubbler could be maintained at room temperature.

Electrical doping was obtained using diethytelluride (DET)† as a 9 ppm mixture in high purity hydrogen for n-type samples, whereas p-type doping was achieved by the addition of diethylzinc (DEZ) from a liquid source. In the case of the DEZ it was also necessary to cool its bubbler to -16°C to enable values of N_a in the range $5x10^{17}$ - 10^{19} cm^{-3} to be obtained.

In addition, the reacting gas mixture was diluted by mixing it with a large excess of hydrogen (~5 l/min) prior to its entering the reaction zone. A complication arises because of the reaction of TEI with AsH_3 at ambient temperatures (17). This reaction leads to the formation

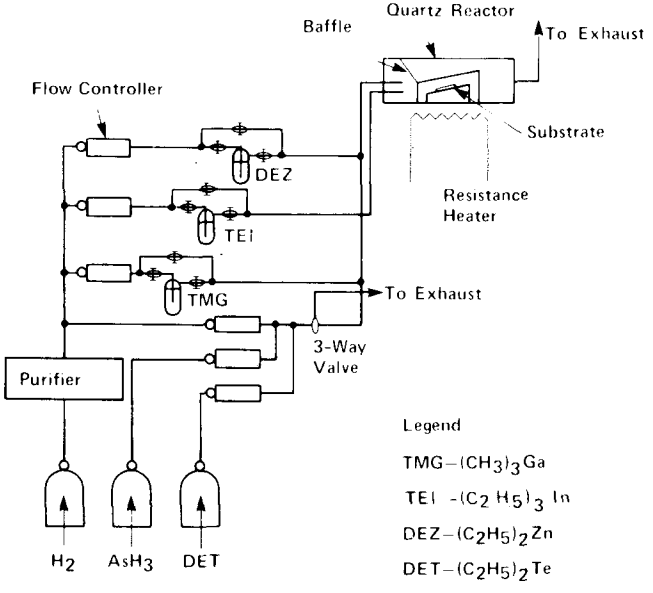

Figure 1. OMP Deposition System Schematic.

†Synthatron Corporation

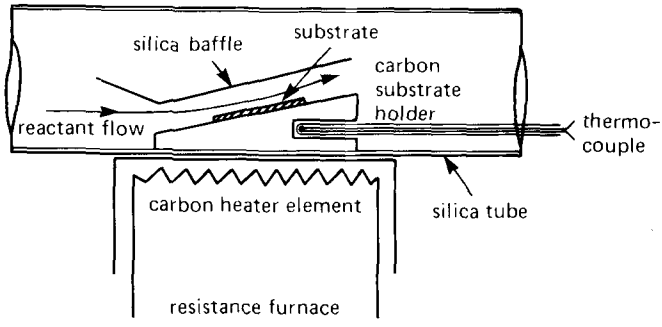

Figure 2. Detail of OMP Heater Assembly and Deposition Zone.

of non-volatile organometallic oils which significantly deplete the gas stream of TEI. In order to overcome this difficulty the TEI gas stream entered the reactor through a separate inlet tube and was mixed with the other gases ~4 cm before entering the heated zone. Even so this still led to some depletion of the TEI, which was observable as a yellowish-brown deposit on the cold walls of the reactor.

The pyrolysis of the gas mixture was achieved by passing it over a heated, angled (8°) carbon block on the surface of which polished GaAs substrate crystals were placed. Details of the deposition zone and heater assembly are shown in Figure 2. Unlike most other deposition systems (15,16,18-20), heating of the deposition zone was carried out indirectly by means of an external, flat, carbon meander resistance heater. 900 W power dissipation in this heater was sufficient to raise the upper surface of the angled carbon block to a temperature of ~800°C. Excellent temperature uniformity was obtained over an area of ~10 cm^2 and the temperature could be controlled to better than ±0.5°C.

The gas mixture was constrained to flow in an essentially laminar manner over the surface of the angled block by means of a quartz baffle. The spacing from the carbon block at the rear of the baffle was lower than at the front which resulted in a concentration of the gas mixture towards the rear, and compensated, to some extent,

for material depletion. This enabled more uniform thickness, homogeneous composition, layers to be prepared.

b) GaAs Epitaxial Growth

Initial experience with the OMP deposition system was obtained by establishing the conditions for the growth of GaAs on Si-doped (n-type) and Cr-doped (semi-insulating) (100) GaAs substrates. In common with previous reports of OMP-GaAs it was observed that both the surface morphology and the electrical properties of the grown layer were strongly dependent on the relative amounts of gallium and arsenic present in the gas stream (20-23). For [As]/[Ga] $\leq$ 4-6:1 the undoped layers were p-type with a relatively poor surface. However, as the ratio was increased beyond 8:1 the layers became n-type with an essentially featureless surface morphology. The lowest values of undoped carrier concentration ($\leq 10^{15} cm^{-3}$), together with the smoothest epitaxial surfaces, were found for [As]/[Ga] ratios of ~12:1. Optimum growth temperature for GaAs was in the range 675 - 725°C. Typical growth conditions for an undoped layer were a flow of 3.0 cm^3/min of H_2 through the TMG bubbler (0°C), 66 cm^3/min AsH_3 (5% in H_2), a diluting carrier gas flow of 2.5 l/min H_2 and a growth temperature of 700°C. Under these conditions growth rates were ~0.15 μm/min.

Excellent control over n-type doping was obtained using DET (9 ppm in H_2) for doping levels in the range 5×10^{16} - 2×10^{18} cm^{-3}. Photoluminescence intensities of typical epitaxial layers at 300 K were comparable to those obtained from LPE GaAs of equivalent doping level. The high vapour pressure of DEZ made it difficult to achieve very low acceptor levels. Typically, acceptor concentrations in the range 5×10^{17} - 2×10^{19} cm^{-3} could be obtained. Nevertheless, it was possible to prepare abrupt p-n junction structures, with epitaxial n and p layers (~3 μm each). These structures, when fabricated into large area LED's, had external quantum efficiencies as high as 1%. Such values are comparable to those obtained for conventional Zn-diffused LED's.

On the basis of the above results, it was concluded that the OMP deposition system was capable of yielding epitaxial GaAs of optoelectronic device quality. By adding

an indium source (TEI) the investigation was then extended to the preparation and evaluation of GaInAs alloy structures.

c) $Ga_{1-x}In_xAs$ Epitaxial Growth

The deposition conditions established by Baliga and Ghandi (17) were used as a starting point for this investigation, and epitaxial layers of $Ga_{1-x}In_xAs$ were prepared with values of indium fraction (x) in the range 0-0.3. Because of flow capacity limitations of the hydrogen purifier, a lower flow of diluting carrier gas was used (~5 l/min), but this did not affect the optimum deposition temperature of ~600°C. As with the previous work (17) a linear relationship between the TEI bubbler flow rate and x was found, Figure 3, for a fixed flow rate through the TMG bubbler. However, the line in Figure 3 is displaced from the origin by ~80 cm^3/min TEI flow.

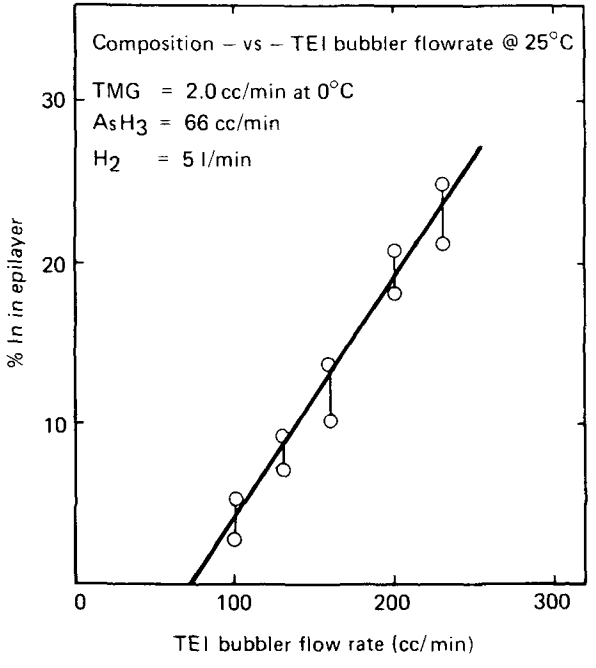

Figure 3. Indium Content of Epitaxial Layers as a Function of TEI Bubbler Flow Rate.

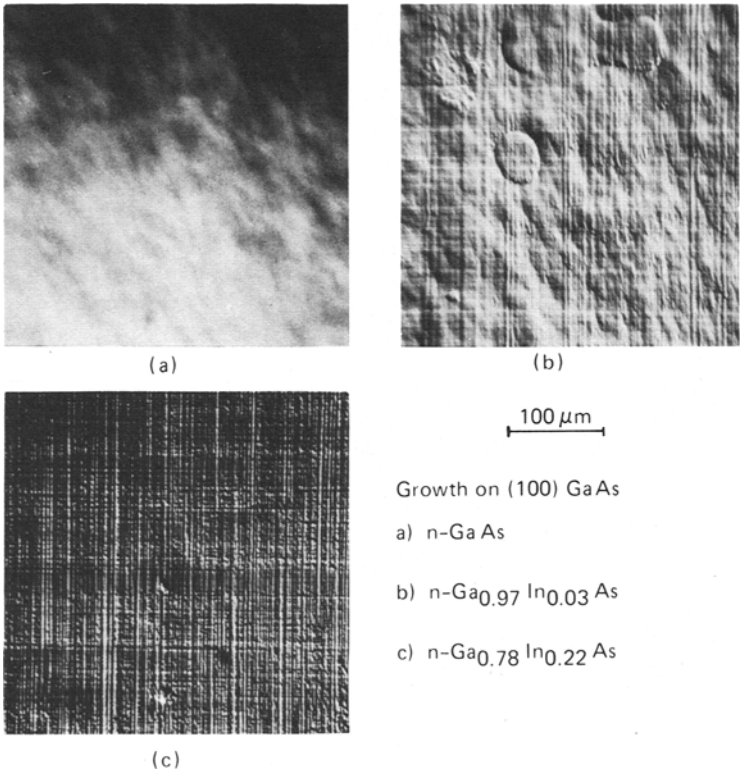

Figure 4. $Ga_{1-x}In_xAs$ Epitaxial Layers on (100) GaAs.

This displacement is attributable to the loss of TEI by reaction with AsH_3 before the gas mixture entered the deposition zone:-as mentioned before, the products of this reaction are visible as a yellowish-brown deposit on the up-stream walls of the reactor. To reduce this loss is would be necessary to increase the carrier gas flow significantly and/or place the exit of the TEI carrier tube closer to the heated zone.

For the deposition conditions described in Figure 3, typical growth rates were 0.035-0.045 μm/min and 4 μm layers were grown over a two hour period for evaluation purposes. Additionally, they were usually doped n-type at the 5×10^{17} - 10^{18} carriers cm^{-3} level.

The surfaces of the grown layers were generally mirror smooth to the naked eye. However, on microscopic examination the typical orthogonal [110] cross-hatch network due to mismatch dislocation could generally be seen. Typical surfaces for (100) orientation epitaxial layers are shown in Figure 4. With increasing indium content the epitaxial surfaces also became microscopically rougher, Figure 4 c). This tendency towards rougher surfaces could be reduced, to a certain extent, by growing on off-orientation substrates. The optimum misorientated substrate surface, in common with the vapour-phase deposition of many semiconductor materials, was found to be 2-3° from (100) towards (110); a value of 3° off was selected for the majority of epitaxial growth runs. The improvement in surface quality due to the use of misoriented substrates can be seen in the upper photographs of Figure 5; the two crystals in the figure were prepared simultaneously, side-by-side, in the same deposition run.

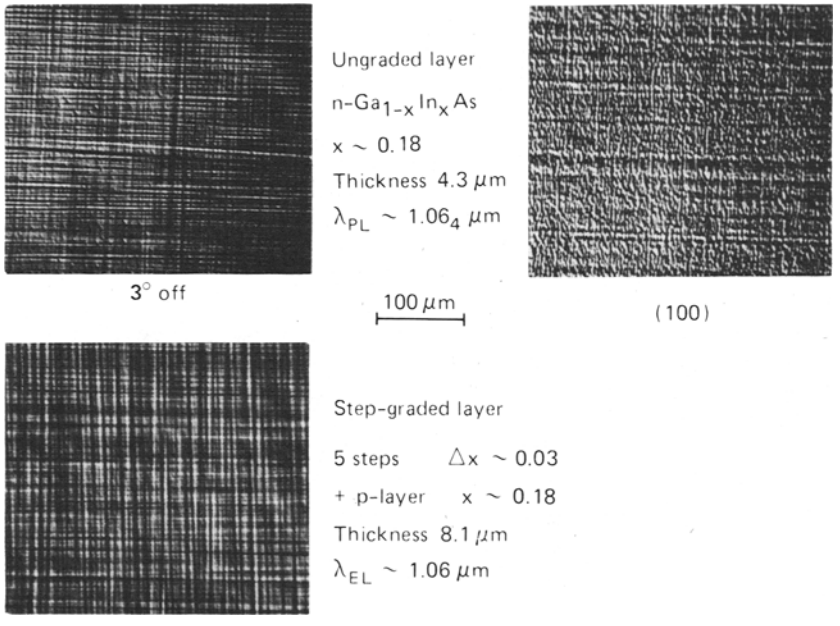

Figure 5. Comparison of $Ga_{1-x}In_xAs$ Epitaxial Layers
a) 3° off-orientation, b) on-orientation,
c) step-graded layer on 3° off orientation GaAs.

Attempts were also made to reduce the misfit dislocation density by preparing step-graded layers (2). The results of one of these attempts is shown as the lower photograph in Figure 5. For this particular crystal the surface composition ($x \sim 0.18$) was arrived at after five steps with $\Delta x \sim 0.03$, and a final layer of p-type $Ga_{0.82}In_{0.18}As$ was also deposited. There is some reduction in misfit dislocation density for this structure when compared to the ungraded layer in the upper photograph of Figure 5. It is recognized that significant further reductions in misfit dislocation density will necessitate the deposition of step-graded epitaxial layers with more closely spaced steps; e.g. $\Delta x \sim 0.01/\mu m$ (5). However, for the low growth rates presently attained, prohibitively long deposition runs are required for $x \geq 0.10$. Consequently, the majority of epitaxial layers deposited in this investigation did not benefit from step-grading.

Epitaxial Layer Characterisation

Composition - x

The epitaxial layer compositions were determined using a variety of methods. These included photoluminescence, optical transmission, electroreflectance and x-ray diffractometry. The optical methods used provided a measure of the direct bandgap (E_g) of the alloys and were generally in excellent agreement with one another. Photoluminescence intensities for GaAs epitaxial layers were essentially the same as those obtained for LPE material of comparable doping level. As the indium content of the alloys was increased, however, the photoluminescence intensities increased above the value for GaAs. This may have been due to the rougher surfaces of the alloys enabling a more efficient extraction of the luminescence, but may also be due to a reduction in the surface recombination with increasing indium content.

In order to convert the measured E_g values to alloy composition it was necessary to assume a form for the variation of E_g with x. Although E_g values are well established for GaAs and InAs, there is still some uncertainty as to the variation of E_g with x. From photoresponse measurements on electrolyte - GaInAs junctions, formed on epitaxial OMP epitaxial layer

surfaces, Baliga et al (26) suggest the strictly linear relationship

$$E_g = 0.36 + 1.005\ (1-x). \qquad (2)$$

Nahory et al (27), however, derive a quadratic relationship of the form

$$E_g = 0.36 + 0.629\ (1-x) + 0.436\ (1-x)^2 \qquad (3)$$

from photoluminescence data obtained on LPE material. Thus very large differences in x can arise in choosing between the linear and quadratic variations in E_g.

It is well established that the variation of lattice parameter (a_0) of $Ga_{1-x}In_xAs$ alloys is linear in x (23). Thus x-ray diffraction measurements of a_0 should enable unambiguous compositional assignments to be made. Unfortunately, lattice deformation resulting from elastic strain and misfit deformation (25) can make precise a_0 measurement difficult to obtain. Nevertheless, approximate value of a_0 could be obtained, and these were combined with the optical E_g value to generate Figure 6. In the figure the solid lines are the linear and quadratic variations of E_g with x. It is clear that the experimental points follow the quadratic form and hence, compositional assignments could be made using Eqn. 3.

Electrical Properties

Electrical characterisation was carried out on single epitaxial layers which were deposited on on-orientation (100) Cr-doped GaAs substrates. A conventional van der Pauw geometry was used with alloyed Sn and In-5%Zn contacts for n- and p-type layers respectively.

The efficiency of incorporation of the doping elements (Te and Zn) was found to be essentially the same as for GaAs: i.e. for the same gas flows from the doping sources similar doping levels were obtained.

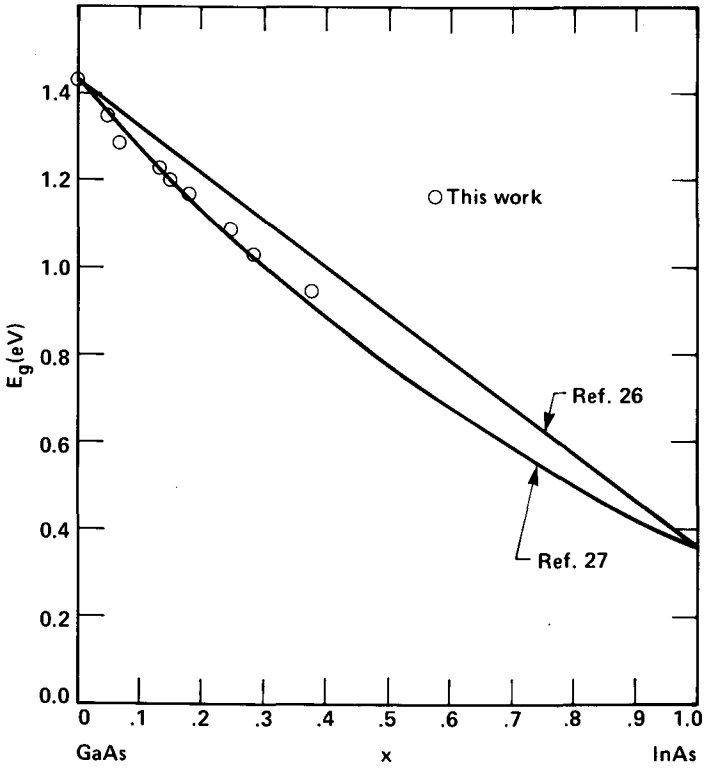

Figure 6. Variation of E_g with Alloy Composition.

Since LED applications required carrier concentrations $\geq 5 \times 10^{17} cm^{-3}$, little work was carried out on undoped layers. However, those that were prepared were n-type, with carrier concentrations (N_d) of $5 \times 10^{16} cm^{-3}$ and mobilities of ~5000 cm^2/volt sec at 300 K.

Intentionally doped n-type layers ($x \leq 0.3$) were prepared with N_d in the range 5×10^{17} - $2 \times 10^{18} cm^{-3}$. These, 3-4 μm thick, layers had 300 K mobilities of 2500-3500 cm^2/volt sec.; values which are considerably higher than the figures reported by Baliga and Ghandi (17) for undoped OMP $Ga_{1-x}In_xAs$ layers (1-2 μm thick). The variations of mobility with alloy composition for n-type epitaxial layers is illustrated in Figure 7. In the figure, mobility values have been normalised to a

carrier concentration of 5 x $10^{17}cm^{-3}$. It has also been assumed that the mobility variation with carrier concentration is essentially the same as that for GaAs (28,29). With this assumption the mobility was found to be essentially independent of x, in agreement with work on CVD $Ga_{1-x}In_xAs$ by Glicksman et al (30) but, again, contrary to the data of Baliga and Ghandi (17).

The electrical characteristics of p-type single epitaxial layers ($x \leq 0.3$) were similar to those of GaAs; e.g. a typical layer with $x \sim 0.2$ and $N_a \sim 5x10^{18}cm^{-3}$ had a hole mobility of 80 cm^2/volt sec.

$Ga_{1-x}In_xAs$ Homojunction LED's

Fabrication

p-n homojunction LED structures were prepared in two ways;

i) by growth of a p-type epitaxial layer on top of n-type $Ga_{1-x}In_xAs$ in the same deposition run, and

ii) by diffusion of Zn into n-type $Ga_{1-x}In_xAs$.

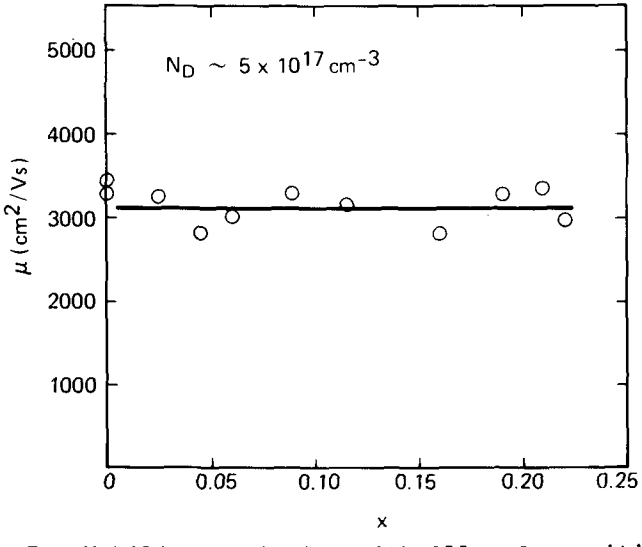

Figure 7. Mobility Variation with Alloy Composition.

The Zn-diffusion technique was used to prepare restricted emitting area LED's compatible with optical fibre core dimensions, whereas the grown p-n junctions were evaluated as large area devices. Since the results for both were qualitatively similar, only the Zn-diffused devices will be described in detail.

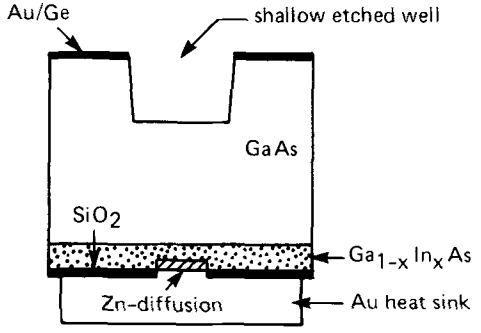

Figure 8.

Cross-section of Zn-diffused LED structure.

A cross-sectional representation of the Zn-diffused device is shown in Figure 8, and is basically similar to that of the Burrus LED structure (31). However, since the substrate material is essentially transparent to the emission from the alloys, for $x > 0.05$, it was not necessary to etch a deep hole in the n-side of the devices. Although a hole, 50-75 μm deep, was generally etched to assist with fibre location.

Zinc-diffusion was carried out at 600°C through 50-75 μm diameter windows photoengraved in 2000 Å of CVD SiO_2 deposited on the $Ga_{1-x}In_xAs$ epitaxial surface. A semi-sealed (box) diffusion capsule (32) was used, with a charge composed of 33% Zn in gallium, together with an equivalent quantity of crushed polycrystalline GaAs. Because of the rapid increase in the Zn-diffusion coefficient with increase in x (33), it was necessary to individually adjust the diffusion times (0.5 - 2 hr.) in order to produce a junction approximately at the mid-point of each epitaxial layer (1.5 - 2 μm deep).

Although the described technique was adequate for providing devices for initial evaluation purposes the devices, so produced, cannot be considered to have been optimised in any way.

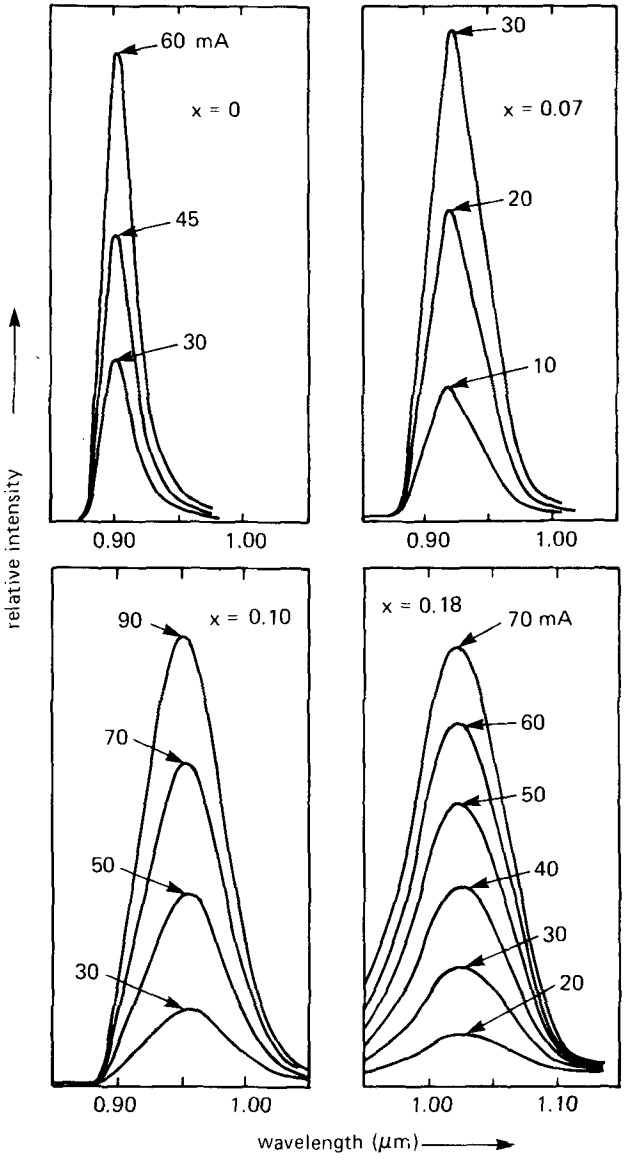

Figure 9. Emission Spectra of Zn-diffused $Ga_{1-x}In_xAs$ LED's.

Evaluation

Conventional emission spectra, current-voltage (I-V) and light output-current (L-I) data were obtained for the diodes. Emission spectra of some representative LED's are shown in Figure 9. However, they have not been corrected for the response of the S1 photocathode. For corrected spectra, the spectral width increased from ~500 Å for low values of x to ~1000 Å for x = 0.25 (1.15 μm spectral peak). (The narrow spectrum of the GaAs device in Figure 9 is due to internal absorption of the short wavelength side of the emission by the substrate). Bandgap values, for the alloys, derived from the corrected spectral peaks, agreed well with those obtained from photoluminescence, optical transmission and electroreflectance measurements on the same epitaxial layers before device processing.

Log-log L-I characteristics of two typical LEDs are shown in Figure 10, one of which was prepared from GaAs and the other from $Ga_{0.83}In_{0.17}As$ (1.04 μm emission). At high current levels both diodes have an approximately linear L-I relationship, with near unity slope. This corresponds to a regime in which carrier injection across the space-charge layer (SCL) dominates current flow and there is a one-to one correspondence between injected charge and light emission; however, only a small fraction of the injected carriers recombine radiatively. As the current is decreased, the slope of the log-log L-I characteristic increases and approaches a value of two at low current levels. Following Kressel and Butler (34); if non-radiative recombination due to defects within the SCL dominates current flow, a current dependence of the form $I \propto \exp(eV/2KT)$ results. However, the light output remains proportional to carrier injection across the SCL, varying as $L \propto \exp(eV/KT)$. Hence, $L \propto I^2$ and a log-log LI plot will have a slope of two. The curve corresponding to the $Ga_{0.83}In_{0.17}As$ LED in Figure 10 clearly illustrates the two regimes. For currents ≥100 mA the light output is proportional to the current. The slope is less than unity, and this may reflect non-radiative recombination at defects outside the SCL. Below 100 mA, however, the effects of defects in the SCL become apparent. For currents less than 30 mA the slope of two is seen. The effect of defects is

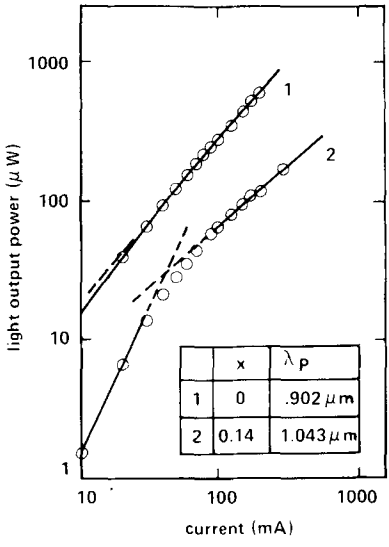

Figure 10. Log-Log L-I Characteristics of Representative LED's.

much less apparent for the GaAs device in Figure 10 and the slope of two is only seen at much lower current levels than are represented in the diagram.

External quantum efficiences (η) of the devices were measured with a calibrated Si-solar cell placed in close proximity. Measured values of η decreased rapidly with increasing x for current levels in the unity slope range of Figure 10. For GaAs (x = 0) typical values of η were in the range 0.3 - 0.4%; a somewhat lower figure than that obtained for broad-area devices because of absorption in the substrate. Whereas for x = 0.25 η was ~0.02% for the best devices.

Values of η for the alloys were significantly lower than those obtained for CVD material (35). This was due undoubtedly, in part, to the lack of grading in the epitaxial layers and the associated high defect densities. A close examination of the p-n junction in cleaved sections through the LED's showed a significant number of narrow, 1 μm wide, diffusion spikes penetrating 2-3 times deeper than the envelope of the main diffusion front. The spike density increased with increasing x and, in many cases, the spikes terminated at the substrate

epitaxial layer interface. Thus, it is not surprising that the device efficiencies were low, since the major deviations from the planar junction interface would contribute significantly to non-radiative leakage currents. Improvements in junction planarity can be expected in carefully graded structures, and this should result in higher efficiency devices.

In spite of the high defect densities and low device efficiencies preliminary 300 K life testing at 2KA/cm^2 established device lifetimes in excess of several hundred hours. These results offer some encouragement in anticipating that improved optimised device structures prepared from OMP material will have acceptable lifetimes for systems applications.

Conclusion

Epitaxial layers of $Ga_{1-x}In_xAs$, with reasonable electrical and optical properties, can be deposited on (100) GaAs substrates using the technique of organo-metallic pyrolysis. Homojunction, zinc-diffused, LED's prepared in such epitaxial materials have decreasing external quantum efficiencies with increasing indium content. This decrease can be attributed to the lack of grading in the epitaxial layers, which results in high defect densities in the junction region. To prepare graded structures will, however, involve increasing the present low growth rate so that suitable grading schemes can be implemented in acceptable deposition times.

Acknowledgements

The authors would like to thank Prof. J.C. Woolley and Mr. J. Goodchild of Ottawa University for carrying out electroreflectance measurements. The work presented in this paper was partially supported by the Canadian Government as part of the Industrial Research Assistance Program.

References

1) Conradi J., Kapron F.P. and Dyment J.C., IEEE Trans. Electron Devices ED-25, 180(1978).

2) Nuese C.J., J. Electron. Mater. 6, 253(1977).
3) Hsieh J.J., J. Electron. Mater. 7, 31(1977).
4) Goodfellow R.C., Carter A.C., Griffith I., and Bradley R.R., IEEE Trans. Electron. Devices ED-26, 1215(1979).
5) Mabbitt A.W. and Mobsby C.D., Electron. Lett. 11, 158(1975).
6) Pearsall T.P. and Papuchon M., Appl. Phys. Lett. 33, 640(1978).
7) Miller B.I., and McFee J.H., J. Electrochem. Soc. 125, 1310(1978).
8) Nagai H. and Noguchi Y., J. Appl. Phys. 49, 450(1978).
9) Manasevit H.M. and Simpson W.I., J. Electrochem. Soc. 116, 1725(1969).
10) Umebachi S., Asahi K., Inoue M. and Kano G., IEEE Trans. Electron. Devices ED-21, 613(1975).
11) Dupuis R.D., Dapkus P.D., Yingling R.D. and Moudy L.A., Appl. Phys. Lett. 31, 201(1977).
12) Nelson N.J., Johnson K.K., Moon R.L., Vander Plas H.A. and James L.W., App. Phys. Lett. 33, 26(1978).
13) Dupuis R.D. and Dapkus P.D., Appl. Phys. Lett. 31, 466(1977).
14) Thrush E.J., Selway P.R. and Henshall G.D., Electron. Lett. 15, 157(1979).
15) Bass S.J., J. Cryst. Growth 31, 172(1975).
16) Manasevit H.M. and Simpson W.I., J. Electrochem. Soc. 116, 1725(1969).
17) Baliga B.J. and Ghandi S.K., J. Electrochem. Soc. 122, 683(1975).
18) Dupuis R.D. and Dapkus P.E., IEEE J. Quantum Electron. QE-15, 128(1979).
19) Stringfellow G.B. and Horn G., Appl. Phys. Lett. 34, 794(1979).
20) Andre J.P., Gallais A. and Hallais J., Inst. Phys. Conf., Series No. 33a, 1(1977).
21) Stringfellow G.B., Ann. Rev. Mater. Sci. 8, 73(1978).
22) Bass S.J. and Oliver P.E., paper presented at 1976 North American Symposium on GaAs and Related Compounds, St. Louis, Missouri.
23) Ito S., Shinohara T. and Seki Y., J. Electrochem. Soc. 120, 1419(1973).
24) Woolley J.C. and Smith B.A., Proc. Phys. Soc. (London) B70, 153(1957).

25) Nagai H., J. Appl. Phys. 45, 3789(1974)
26) Baliga B.J., Bhat R. and Ghandi S.K., J. Appl. Phys. 46, 4608(1975).
27) Nahory R.E., Pollack M.A., Johnston W.D., and Barns R.L., Appl. Phys. Lett. 33, 659(1978).
28) Sze S.M., "Physics of Semiconductor Devices", Wiley-Interscience, (1969).
29) Rode D.L. and Knight S., Phys. Rev. B 3, 2534(1971).
30) Glicksman M., Enstrom R.E., Mittleman S.A. and Appert J.R., Phys. Rev. B. 9, 1621(1974).
31) Burrus C.A. and Miller B.I., Opt. Commun. 4, 307(1971).
32) D'Asaro L.A., Solid State Electron. 1, 3(1960).
33) Noad J.P. and SpringThorpe A.J., to be published
34) Kressel H. and Butler J.K., "Semiconductor Lasers and Heterojunction LED's", Academic Press. p. 71, (1977).
35) Mabbitt A.W. and Goodfellow R.C., Electron. Lett. 11, 274(1975).